Determination of Ion Cluster Sizes and Cluster-to-Cluster Distances in Ionomers by Four-Pulse Double Electron Electron Resonance Spectroscopy

M. Pannier, V. Schädler, M. Schöps, U. Wiesner,† G. Jeschke, and H. W. Spiess*

Max-Planck-Institut für Polymerforschung, Postfach 3148, D-55021 Mainz, Germany

Received May 9, 2000

ABSTRACT: Double electron−electron resonance (DEER) spectroscopy is introduced as a new tool for the characterization of mesoscopic structures in polymers. This method can characterize distance distributions between spin probes in a range between 1.5 and 8 nm and can be applied to the measurement of ion cluster sizes and intercluster distances in ionically end-capped polymers by using ionic spin probes that attach themselves to the surface of the ion clusters. The results on intercluster distances for systems based on homopolymers are in agreement with earlier results from small-angle X-ray scattering (SAXS), while the cluster sizes can be rationalized by comparison with a force field molecular model of an ion cluster. The DEER experiment could also be applied to an ionically end-capped diblock copolymer for which a SAXS measurement of the intercluster distance failed.

Introduction

Structure formation on nanoscopic length scales by self-assembly of molecules is of great current interest in both materials science[1,2] and biology.[3] Classical scattering methods fail in the characterization of distance distributions in such structures if the materials do not feature substantial long-range or at least medium-range order. They may also fail with increasing complexity of the materials because of strong overlap of peaks due to different structural features. For instance, we were recently able to estimate distances between ion multiplets (clusters) in ionically end-capped homopolymers by small-angle X-ray scattering (SAXS),[4] but could not extend this methodology to ion multiplets in similar diblock copolymers where the SAXS profiles are dominated by block copolymer peaks. This is rather disappointing, as the ionic clusters play a decisive role in the structure formation and in particular for the molecular dynamics.[5] Local methods such as magnetic resonance spectroscopy should be able to overcome these problems, as they can characterize even broad distance distributions by separating the distance-dependent dipole−dipole interaction between spins from all other interactions. In addition, sufficient contrast can be obtained in most cases by a judicious choice of the observer spins.[6] For measurements of distances above 1 nm, as in the above-mentioned ionomers, electron paramagnetic resonance (EPR) spectroscopy appears to be better suited than NMR spectroscopy because of the magnetic moment of electron spins being 680 times larger than the one of the nuclei with largest magnetogyric ratio (protons). We have demonstrated recently that the four-pulse double electron−electron resonance (DEER) experiment can be used for precise distance measurements at least up to 3 nm and have presented a first result for an ionomer.[7,8]

In the present work we introduce four-pulse DEER as a tool for the characterization of ion clusters and their distribution in end-capped polymers. We show that the time-domain DEER signal of the ionomers consists of three components that can be modeled by two Gaussian distance distributions with mean values of about 1.5−2 and 4−7 nm and a uniformly distributed background. The Gaussian component at about 2 nm is a measure of the cluster size while the Gaussian component at 6−7 nm corresponds to intercluster distances. The results are in semiquantitative agreement with SAXS data concerning intercluster distances and with molecular force field calculations concerning cluster sizes. Experimental evidence is provided for an attachment of the ionic spin probes to the surface of the ion clusters. The intercluster distance in poly(isoprene) with quaternary ammonium end groups is found to increase with increasing molecular weight. Similar mean sizes and distances are found for poly(isoprene) with sulfonate end groups and a poly(styrene)−poly(isoprene) diblock copolymer with sulfonate end groups on the poly(isoprene) chains.

Experimental Section

Sample Preparation and Characterization. End-capped poly(isoprene) and poly(styrene) homopolymers and poly(styrene)−poly(isoprene) diblock copolymers were prepared by anionic polymerization and subsequent introduction of the ionic end groups.[4,10] All samples with a given molecular weight but different end groups were derived from the same polymerization batch, thus ensuring identical molecular weight distributions and stereochemistry of the poly(isoprene) chain. Sample characterization has been described elsewhere.[4,5] The spin probes 4-carboxy−TEMPO, 5-DOXYL−stearic acid and 12-DOXYL−stearic acid were converted to their potassium salts (K-TEMPO, K-5-DS, K-12-DS) by titration with 0.1 mM methanolic KOH. The biradical 2,6-bis[(((2,2,5,5-tetramethyl-1-oxypyrrolin-3-yl)carbonyl)oxy]anthrachinon (BPA) was synthesized as described by Larsen and Singel.[9] The samples for DEER studies were prepared by solvent casting: 100 mg of the polymer was dissolved in 10 mL of toluene and mixed with the calculated amount of 0.05% methanolic spin probe solution such that the ratio of spin probes per ionic chain ends was 2/15. After film casting and solvent evaporation the samples were dried and annealed under vacuum at 120 °C for more than 6 h, before being transferred to the EPR tube. The ionomers studied in this work are shown in a schematic representation in Figure 1 together with the structures of the

† Present address: Materials Science & Engineering, Cornell University, 329 Bard Hall, Ithaca, NY 14853-1501.

10.1021/ma000800u CCC: $19.00
Published on Web 10/03/2000

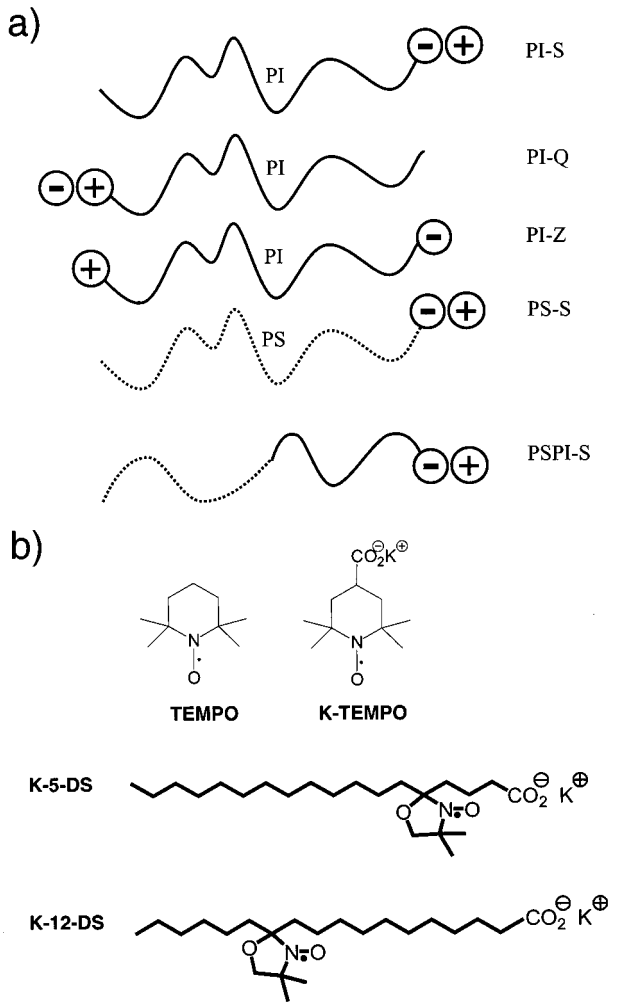

Figure 1. Schematic representation of the investigated ionomers (a) and chemical structures of the spin probes (b).

Table 1. Molecular Characteristics of the Investigated Polymers

sample	PI-Q10	PI-S10	PI-Z10	PS-S5	PI-Q16	PS-PI-S24
M_n (kg/mol)	10	10	10	4.8	16	24[a]
M_w/M_n	1.07	1.07	1.07	1.07	1.08	1.08

[a] M_n(PS) = 12.7 kg/mol.

Table 2. DEER and SAXS Distances of the Investigated Polymers

sample	PI-Q10	PI-S10	PI-Z10	PS-S5	PI-Q16	PS-PI-S24
r_1^{DEER}/nm[a]	1.8	1.9	1.8	1.4	2.2	2.22
$\sigma(r_1^{DEER})$/nm	0.47	0.76	0.43	0.47	0.43	0.49
r_2^{DEER}/nm[b]	5.4	5.0	4.7	4.4	6.6	6.31
$\sigma(r_2^{DEER})$/nm	1.03	1.16	1.18	1.29	0.98	0.72
r_2^{SAXS}/nm[b,c]	7.1	6.7	5.7			

[a] Assigned to cluster size. [b] Assigned to intercluster distance. [c] From ref 4.

spin probes. The molecular characteristics are given in Table 1.

EPR Spectroscopy. EPR spectra were measured at a Bruker ESP 380E pulse EPR spectrometer (X-band, ca. 9.7 GHz) equipped with an ENDOR probehead EN 4118X-MD-4 (Bruker). The resonator was overcoupled to $Q_L \approx 100$ to provide for a bandwidth sufficient for the double resonance experiment. Microwave from an external tunable second microwave source (Avantek AV 78012 YIG oscillator customized by Magnettech GmbH, Berlin) was fed to one microwave pulse former unit of the spectrometer. All measurements were performed with liquid helium cooling at a temperature of 15 K at repetition rates of 100 Hz with pulse lengths of 32 ns for all microwave pulses and a difference between pump and observer frequency of 50−70 MHz. The pump position was chosen at the maximum of the nitroxide EPR spectrum.[7]

Molecular Modeling. Force field calculations were performed with the Merck Molecular Force Field[11−13] as implemented in the Spartan software package (Wavefunction Inc.) on a Pentium PC. We first optimized the geometry of a single oligomer chain consisting of two isoprene units, an 1,1-diphenylethene unit, and the *N*,*N*-dimethylbenzylamine end group quaternized with methyl bromide. A cluster of 10 such chains was then built up by adding further chains one by one and optimizing the geometry after each step. Two preoptimized molecules of the hydroxylamine corresponding to K-TEMPO were then added and optimization performed. Finally the oligomer chains were extended by two more monomer units each with geometry optimization being performed after the extension of each chain. During the whole procedure it was checked that strain energies increased only gradually after each step. For determination of the theoretical distance in the biradical BPA, the N−O• groups of the nitroxide moieties were replaced by keto groups as suggested by Hartmann et al.,[14] and the average over the 100 conformations with lowest energy was calculated. The distance was taken as the average of the C−C and O−O distances of the keto group. For the conformation with lowest energy this result differed by less than 0.02 nm from the one of a density functional calculation of the biradical with the B3LYP functional.

Results and Discussion

1. Interpretation and Quantification of DEER Data. Distance measurements by magnetic resonance methods utilize the r^{-3} dependence of the dipole−dipole interaction between two spins. For the DEER experiment on nitroxide spin probes, the high-field approximation applies, only the secular part of the coupling between two electron spins needs to be considered, and the *g* values of both spins can be approximated by the free electron value g_e. In angular frequency units the coupling is then given by

$$\omega_{ee}(\theta) = \frac{g_e^2 \mu_B^2 \mu_0}{4\pi\hbar} \frac{1}{r^3} (3\cos^2\theta - 1) \qquad (1)$$

where μ_B is the Bohr magneton, r the distance between the two spins, and θ the angle between the magnetic field axis and the axis connecting the loci of the two electron spins. In samples lacking macroscopic order, θ is distributed with a weighting $\sin\theta$ between 0 and 90°, so that the dipolar spectrum is a Pake pattern with singularities corresponding to $\theta = 90°$. For distances larger than 1.5 nm, additional exchange contributions to the coupling between the two electron spins can be neglected and the distance can be calculated directly from the frequency $\nu_s = \omega_{ee}(90°)/2\pi$ of the singularities according to

$$r = \left(\frac{52.04\ \text{MHz}}{\nu_s}\right)^{1/3} \text{nm} \qquad (2)$$

For distances above 1.5 nm, dipole−dipole couplings are usually not resolved in EPR spectra. The dipole−dipole coupling can be separated from all other interactions by the three-pulse DEER experiment that measures the frequency change of the transition of an observer spin A caused by flipping a coupled spin B with a microwave pump pulse of a different frequency.[15−17] The DEER time-domain signal is modulated with $\cos(\omega_{ee}t)$ as a function of an interpulse delay t between the first

observer pulse and the pump pulse. In this work, we apply an extended four-pulse version of the DEER experiment that overcomes the restriction of three-pulse DEER to interpulse delays $t > t_d$, where t_d is an instrumental deadtime that is usually of the order of 50 to 100 ns.[7] Only this allows access to broad distributions of distances below 3 nm which otherwise cause a signal decay within the dead time.

1.1. Components of the DEER Signal. Even in the case of fairly well isolated spin pairs, as for instance biradicals diluted in a polymer matrix, the signal due to the spin pairs is superimposed by an exponentially decaying background. This is because the pump pulses are selective with respect to the B spins; i.e., there are A spins whose coupling partners within the biradical (intramolecular partners) are not excited. The exponential decay of the background is caused by excitation of spins in other biradicals (intermolecular partners). The signal is now described by

$$V(t) = \exp(-kCF_B)[1 - \int_0^{90°} \lambda(\theta)(1 - \cos(\omega_{ee}t)) \sin\theta \, d\theta] \quad (3)$$

with

$$k = \frac{2\pi g_e^2 \mu_B^2 \mu_0}{9\sqrt{3}\hbar} \quad (4)$$

where C is the volume concentration of the spin probes, F_B is the fraction of B spins excited by the pump pulse, and λ is a modulation depth parameter that is related to F_B but depends on θ if the orientations of the two radicals are correlated. Note that the exponential decay due to intermolecular couplings also applies to the intramolecular contribution. This leads to an upper limit of accessible distances of about 10 nm for volume concentrations of the spin probes as used in this work. The background can be eliminated by fitting and subtracting an exponential as is shown in Figure 2 for the biradical BPA. The experimental distance of 1.94 nm agrees well with the average theoretical distance of 1.941 nm found by a force field Monte Carlo conformer search.

For the case of several well-defined distances r_i between A and B spins, the factor in square brackets in eq 3 has to be replaced by the product of analogous factors for all the distances with proper weighting factors λ_i. If $\lambda_i \ll 1$ for all pair distances, only terms linear in the λ_i need to be considered. In the case of spin probes in ionomers the orientations of the nitroxide moieties are uncorrelated, so that the λ_i do no longer depend on θ and are all equal. For a continuous distance distribution $G(r)$, the signal can then be closely approximated by

$$V(t) = \exp(-kCF_B)[1 - \int_{r_{min}}^{r_{max}} G(r) \int_0^{90°} (1 - \cos(\omega_{ee}(r,\theta)t)) \sin\theta \, d\theta \, dr] \quad (5)$$

where r_{min} is the minimum distance at which spin pairs can still be excited (about 1.5 nm)[8] and r_{max} is the maximum distance for which the nonuniform part of the distance distribution still contributes significantly to the signal variation with t (about 15 nm).

Any peak in the distance distribution contributes an oscillation to the time-domain signal whose frequency depends on the distance at its maximum according to eq 2 and whose amplitude depends on $G(r)$ at the maximum. The oscillation decays with a rate determined by the width of the peak. Note that the same peak width leads to a faster decay at smaller distances due to the r^{-3} dependence of ω_{ee}. Accordingly, peaks at small distances contribute to the signal only at early times while peaks at large distances influence the long-time behavior of DEER data. For a mean number of two spin probes attached to each ionic cluster, the peaks in the distance distribution due to probe pairs on the same cluster and probe pairs on neighboring clusters are expected to be of similar amplitude. Intercluster distances in ionically end-capped homopolymers are in the range 5−7 nm according to SAXS data,[4] while cluster sizes for a mean number of 15 chain ends per cluster are expected to be significantly smaller. In agreement with these expectations, two additional features are observed in DEER time-domain data for ionic K-TEMPO probes in an ionomer (Figure 3a) as compared to the uniformly distributed hydrophobic TEMPO probes (Figure 3b). Using eq 5, the data for K-TEMPO can be fitted by assuming a distance distribution consisting of two Gaussian peaks (Figure 3d) and the uniform background as shown in Figure 3b. The residual displayed in Figure 3c is made up of noise and weak nuclear modulations from nearby protons that cannot entirely be suppressed in the DEER experiment.[7] The

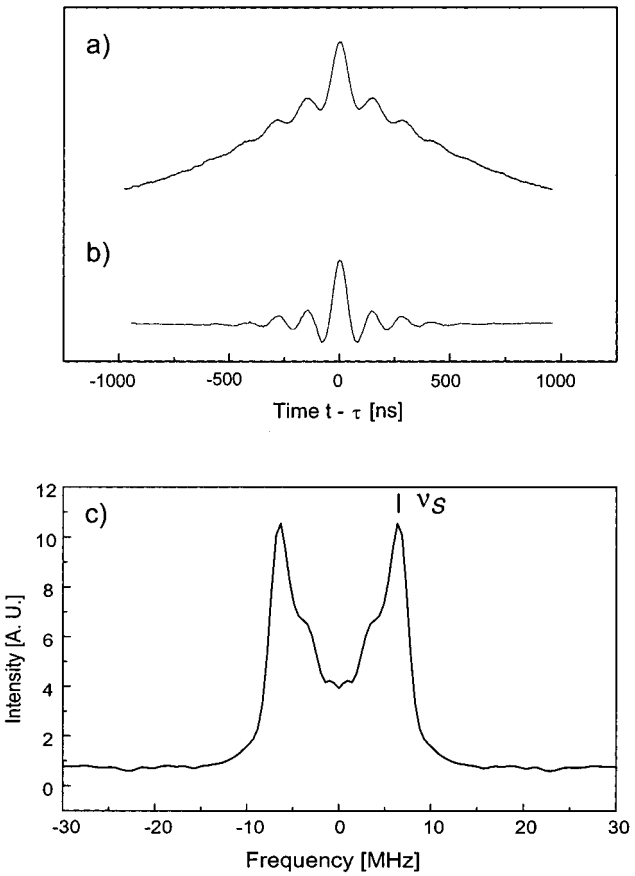

Figure 2. DEER time-domain data and dipolar spectrum for the rigid biradical BPA with a well-defined N−N distance of the nitroxide moieties of 1.89 nm. (a) Original time-domain data. (b) Data after subtraction of the exponential decay function. (c) Dipolar spectrum with a frequency $\nu_S = 7.12$ MHz for the singularities corresponding to a distance of 1.94 nm. The theoretical value for an average over the 256 conformers with lowest energy is 1.941 nm.

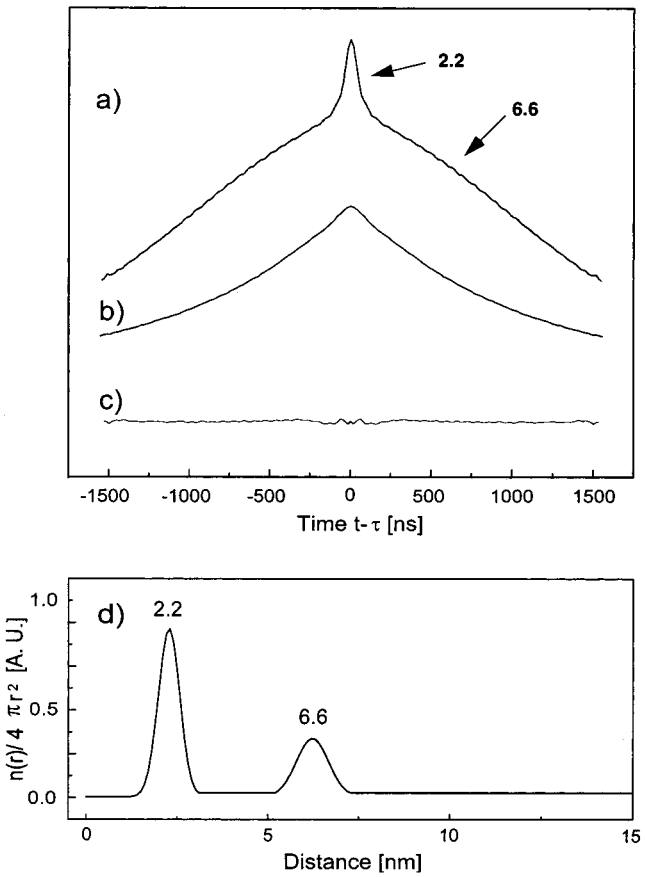

Figure 3. Components and analysis of DEER time-domain data of ionomers. (a) Experimental result for the ionic spin probe K-TEMPO in PI-Q16. (b) Experimental result for the hydrophobic spin probe TEMPO in PI-Q16. (c) Residual of the fit of the data for K-TEMPO according to eq 5. (d) Distance distribution obtained from a fit of the data for K-TEMPO. The most prominent features corresponding to the two peaks of the distribution are marked in part a.

simple distance distribution thus fully accounts for the experimental data and a more elaborate analysis does not seem to be justified.

1.2. Precision of DEER Distances. Interpretation of distance distributions derived from DEER data requires an estimate on the precision to which distances between two spin probes can be determined and considerations how distances between spin probes are related to the characteristic distances in the system of interest (see section 1.3). From the estimated error of 0.1 MHz for the measurement of the dipolar frequency ν_S one obtains a precision of 0.16 nm at $r = 4$ nm. The relative error from this source scales with r^4.

For assessing trends in a series of similar materials, the sensitivity of DEER data to small changes in the distance distribution may be more important than the precision of absolute numbers. The results of a model calculation concerning this question are displayed in Figure 4. A change in the smaller distance from 2 to 2.5 nm leads to a change of the DEER signal at short times that would easily be recognized in experimental data of a quality as obtained in this work (Figure 4a). The same is true for the change in the DEER signal at longer times found after changing the larger distance form 5.0 nm to 5.5 nm (Figure 4b).

1.3. Location of the Spin Probes. In earlier continuous-wave EPR studies we have found that the ionic K-TEMPO spin probe is strongly immobilized as compared to the much less polar but similarly sized TEMPO spin probe in the same ionomer.[4] In particular, in poly(isoprene) with 1,4-microstructure and sulfonate end groups the K-TEMPO probes become mobile at a temperature that is 142 K higher than the DSC glass transition temperature. This finding is strong evidence for an attachment of K-TEMPO to the ionic clusters or its incorporation into the clusters. The occurrence of a distance maximum at about 2 nm in this work suggests surface attachment. However, nitroxide pairs at distances below about 1.5 nm do not contribute to the DEER signal anyway, because of limited excitation bandwidth. Even with larger excitation bandwidth, distances below 1.5 nm cannot be precisely determined from the measurement of electron−electron couplings, because exchange contributions are then significant, so that eq 1 is no longer valid. Further evidence for surface attachment may thus be needed. We therefore compared the position of the lower maximum in the distance distribution for the series of spin probes K-TEMPO, K-5-DS, and K-12-DS with increasing distance of the nitroxide moiety from the ionic group for an ionically endcapped poly(styrene)−poly(isoprene) copolymer with molecular weight of 10 000. Indeed, from the dipolar spectra in Figure 5a we find a shift of this maximum from 2.2 nm for K-TEMPO via 2.5 nm for K-5-DS to 3.0 nm for K-12-DS. This result supports our assumption that the spin probes are attached to the ionic clusters as shown in the cartoon in Figure 5d. Note that the spherical shape of the cluster in this drawing is assumed for simplicity and not due to experimental evidence. The first maximum in the DEER distance distribution can then be used as a measure for the cluster size. The second peak corresponds to next-neighbor distances between clusters; its width cannot be smaller than the average cluster size.

2. Ion Cluster Sizes and Intercluster Distances in Ionomers. 2.1. Comparison of DEER and SAXS Data. DEER time-domain data and fit residuals for the ionomers shown in Figure 1 are presented in Figure 6. The mean distance and variance of the two Gaussian peaks in the distance distribution for each ionomer are given in Table 1 together with the SAXS data for the homopolymers taken from ref 4. For the diblock copolymer PS-PI-S24,[19] no ionomer peak could be found in the SAXS profiles. There are also no features in the SAXS profiles that would allow for an independent determination of the cluster size. This problem is addressed in section 2.2. The DEER data for the series PI-Q10, PI-S10, and PI-Z10 exhibits the same trend of decreasing intercluster distances as the SAXS data, albeit with smaller relative changes. DEER intercluster distances are also systematically lower than the values obtained from the SAXS profiles. Though we cannot exclude the possibility that this is partially due to the overweighting of smaller distances in the r^{-3} averaging of DEER, it should be pointed out that the distance estimates from SAXS profiles are based on the Bragg equation that is not strictly valid for systems lacking long-range order.[18]

On increasing the molecular weight of the polymer chain in PI-Q from 10 to 16 kg·mol^{-1} an increase of the intercluster distance from 5.4 to 6.6 nm is observed. The ratio of 1.22 is in agreement with the ratio of 1.26 expected for the square-root scaling of a Gaussian coil, but data for a larger range of molecular weights would be required to obtain a reliable scaling coefficient. The

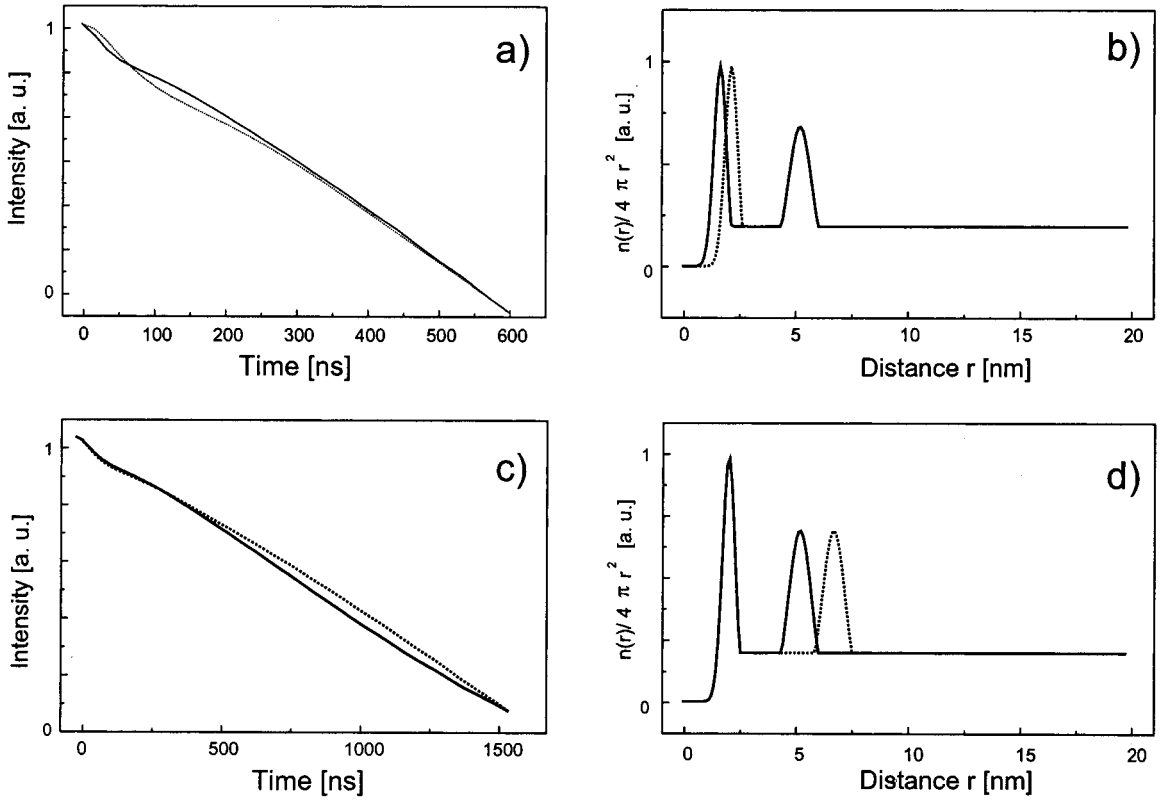

Figure 4. Comparison of DEER time-domain data for slightly different distance distributions (simulations): (a, b) Solid curve, $r_1 = 2.0$ nm, $\sigma(r_1) = 0.4$ nm, $r_2 = 5.0$ nm, $\sigma(r_2) = 1.1$ nm; dashed curve, $r_1 = 2.5$ nm, with the other parameters the same as for the solid curve; (c, d) solid curve, same parameters as in part a; dashed curve, $r_2 = 5.5$ nm, with the other parameters the same as for the solid curve.

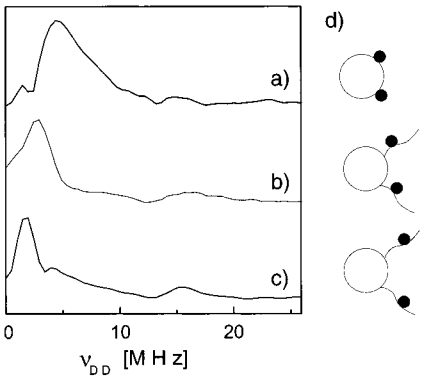

Figure 5. Dipolar spectra for different ionic spin probes in PS-PI-S11 obtained by Fourier transformation of DEER time-domain data after fitting and subtracting the exponentially decaying background: (a) K-TEMPO, $r_1 = (2.2 \pm 0.3)$ nm; (b) K-5-DS, $r_1 = (2.5 \pm 0.3)$ nm; (c) K-12-DS, $r_1 = (3.0 \pm 0.3)$ nm. (d) Cartoon showing the location of the spin probes with respect to the cluster.

differences in cluster size between the different PI ionomers may not be significant, but in PS-S5 the cluster size seems to be reduced, possibly because the bulky aromatic side groups lead to a reduction in the number of aggregating chain ends. The diblock copolymer PS-PI-S24 can be best compared with PI-S10, since the clusters are located in the PI microphase[5] and the length of the PI chains is very similar. Indeed one finds the same cluster size within experimental error, but a larger intercluster distance of 6.31 nm for PS-PI-24 as compared to 5.0 nm for PI-S10. This can be rationalized by the assumption that the PI chains on average feature more stretched conformations in the diblock copolymer. Significant variations in the relative amplitude of the center feature in the EPR signal from spin probes on the same cluster are also apparent in Figure 6. As the mean number n of spin probes per ionic chain end has been kept constant ($n = 2/15$), this can be traced back either to variations in the mean number of chain ends per cluster or in the uniformity of cluster sizes.

2.2. Molecular Modeling of Ionic Clusters. Regarding ion cluster sizes in our samples, no experimental data from other techniques are available for comparison. Ionic domain radii in α,ω-dicarboxylatopoly(butadienes) and α,ω-dicarboxylatopoly(isoprenes) determined by SAXS are in the range from 0.6 to 1.1 nm,[18] i.e., half as large as the "cluster sizes" obtained by DEER for our samples. The analysis of the SAXS data described in ref 18 obtains the domain sizes from the surface-to-volume ratio S/V of the domains manifest in the SAXS profile by assuming a spherical shape of the domains. We have therefore decided to check the consistency of the DEER results with a force field model of the ionic clusters for the case of PI-Q.

Both a tube and a space filling model of a cluster consisting of 10 chains with two surface-attached K-TEMPO probes are displayed in Figure 7. Only two isoprene monomer units per chain are shown for clarity. It has been checked that the cluster structure does not change significantly on extending the chains. Attachment of the spin probes to the surface was assumed based on the experimental results discussed in section 1.3. It also stands to chemical reason that the unpolar part of the spin probe does not penetrate into the core of the ionic cluster in a situation where this can be avoided without compromising the interaction of the

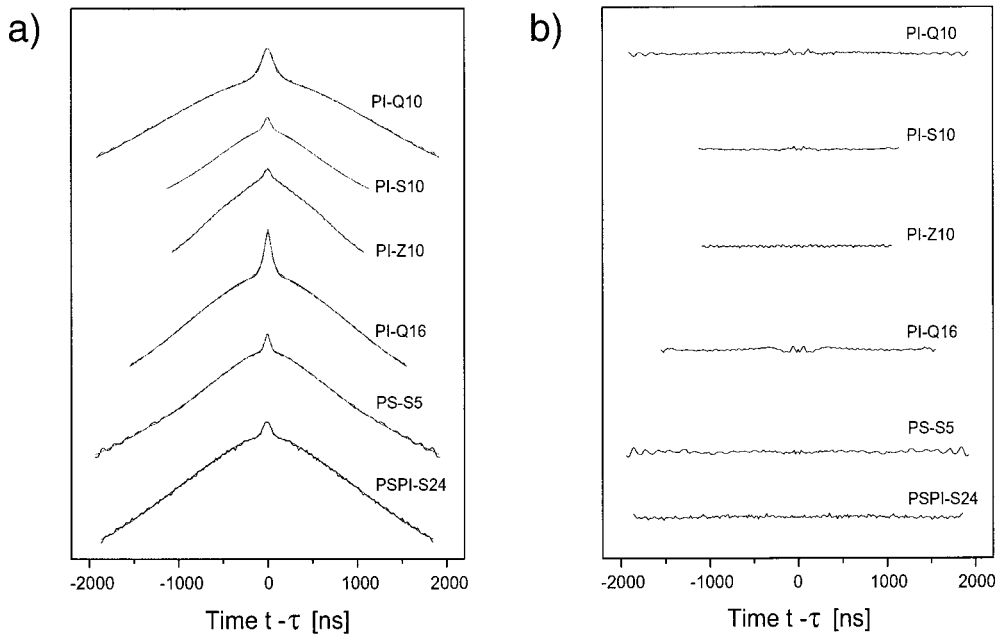

Figure 6. Ionomer DEER time-domain data (a) and fit residuals (b) for the parameters given in Table 2.

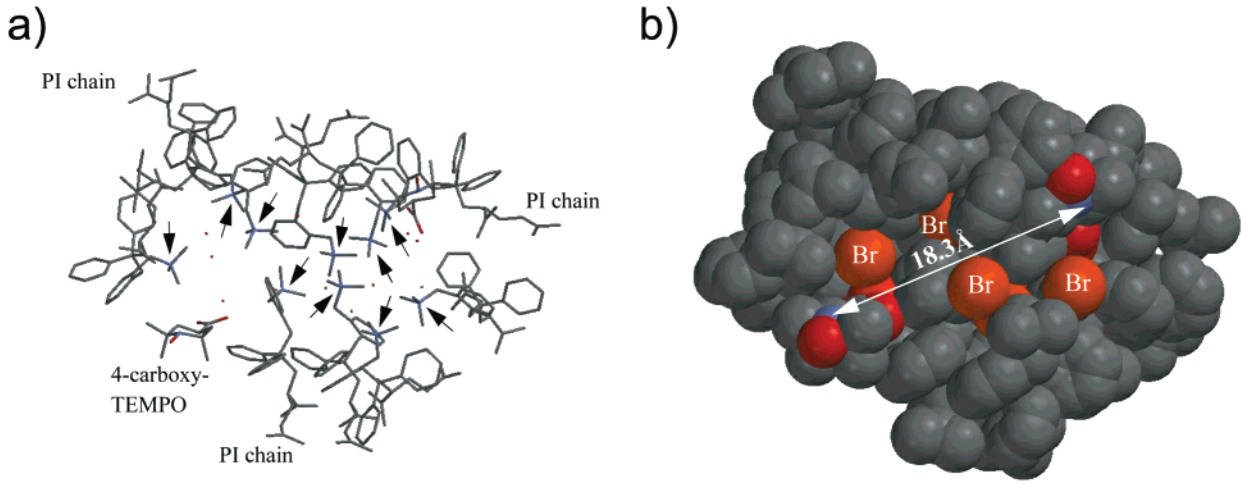

Figure 7. Simulated structure (Merck Molecular Force Field) of a PI-Q model cluster consisting of 10 chains and two attached K-TEMPO spin probes. (a) Tube model. The nitrogen atoms of tetramethylammonium cations are marked by arrows. (b) Space-filling model. Surface-exposed bromide ions are marked and the distance between the nitrogen atoms of the K-TEMPO spin probes is given.

anionic headgroup with cations close to the cluster surface. A distance of about 1.8 nm between nitrogen atoms of the two attached spin probes as shown in Figure 7b is quite typical and is also in agreement with the experimental value of 1.95 nm. After removing all parts of the computed structure that are clearly outside the ionic domain, the model cluster can be approximated by an ellipsoid with half axes of (0.927, 0.802, 0.413) nm. To check the validity of the analysis of the SAXS data concerning cluster sizes, we applied the spherical cluster model to the value $S/V = 10.004$ nm^{-1} for this ellipsoid. This suggests a domain radius of only 0.3 nm which is even smaller than the shortest half axis of the ellipsoid, thus demonstrating that the spherical model applied to SAXS data may lead to a severe underestimation of the size of nonspherical domains.

Conclusion

DEER measurements of distance distributions in the range between 1.5 and 8 nm have been introduced as a new tool for the characterization of mesoscopic structures in polymers. The method does not depend on long-range order for the quantification of next-neighbor distances between spin probes. Measurements on ionomers have been performed by using ionic spin probes that attach themselves to the ion clusters. By using a mean ratio close to two between the spin probes and ion clusters, it is possible to characterize both the cluster size and the intercluster distances. This method has been shown to work also for an ionically end-capped diblock copolymer for which SAXS profiles do not exhibit an ionomer peak. In homopolymers, where SAXS estimates of intercluster distances are available, the corresponding DEER distances are somewhat shorter but show similar trends. The cluster sizes obtained by DEER could be rationalized using a force field model of an ionic cluster. It has been demonstrated that SAXS determination of ion domain radii based on the surface-to-volume ratio and a spherical model may severely underestimate the size of nonspherical clusters. A study

of both α,ω- and μ,ω-ionomers[20] derived from diblock copolymers with different molecular weights and two different morphologies is now in progress.

Acknowledgment. The authors wish to thank R. Ulrich for the synthesis of biradical BPA. Financial support by the DFG Schwerpunkt "Polyelektrolyte" is gratefully acknowledged.

References and Notes

(1) Schlick, L., Ed. *Ionomers: Characterization, Theory, and Applications*; CRC Press: New York, 1996.
(2) Eisenberg, A.; Kim, J.-S. *Introduction to Ionomers*; Wiley-Interscience: New York, 1998.
(3) Barron, A. E.; Zuckermann, R. N. *Curr. Opin. Chem. Biol.* **1999**, *3*, 681.
(4) Schädler, V.; Franck, A.; Wiesner, U.; Spiess, H. W. *Macromolecules* **1997**, *30*, 3832.
(5) Schädler, V.; Kniese, V.; Thurn-Albrecht, T.; Wiesner, U.; Spiess, H. W. *Macromolecules* **1998**, *31*, 4828.
(6) Shin, Y. K.; Levinthal, C.; Levinthal, F.; Hubbel, W. L. *Science* **1993**, *259*, 960.
(7) Pannier, M.; Veit, S.; Godt, A.; Jeschke, G.; Spiess, H. W. *J. Magn. Reson.* **2000**, *142*, 331.
(8) Martin, R. E.; Pannier, M.; Diederich, F.; Gramlich, V.; Hubrich, M.; Spiess, H. W. *Angew. Chem., Int. Ed. Engl.* **1998**, *37*, 2834.
(9) Larsen, R. G.; Singel, D. J. *J. Chem. Phys.* **1993**, *98*, 5134.
(10) Schädler, V.; Spickermann, J.; Räder, H. J.; Wiesner, U. *Macromolecules* **1996**, *29*, 4865.
(11) Halgren, T. A. *J. Comput. Chem.* **1996**, *17*, 490, 520, 553.
(12) Halgren, T. A.; Nachbar, R. B. *J. Comput. Chem.* **1996**, *17*, 587.
(13) Halgren, T. A. *J. Comput. Chem.* **1996**, *17*, 616.
(14) Hartmann, D.; Philipp, R.; Schmadel, K.; Birktoft, J. J.; Banaszak, L. J.; Trommer, W. E *Biochemistry* **1991**, *30*, 2782.
(15) Milov, A. D.; Salikhov, K. M.; Shirov, M. D. *Fiz. Tverd. Tela (Leningrad)* **1981**, *23*, 975.
(16) Milov, A. D.; Ponomarev, A. B.; Tsvetkov, Y. D. *Chem. Phys. Lett.* **1984**, *110*, 67.
(17) Milov, A. D.; Maryasov, A. G.; Tsvetkov, Y. D. *Appl. Magn. Reson.* **1998**, *15*, 107.
(18) Williams, C. E.; Russell, T. P.; Jérôme, R.; Horrion, J. *Macromolecules*, **1986**, *19*, 2877.
(19) This sample has been labeled S24 in ref 5.
(20) Schöps, M.; Leist, H.; Du Chesne, A.; Wiesner, U. *Macromolecules* **1999**, *32*, 2806.

MA000800U